ME 51 Labs 3 & 4 Report

Air Cooling of Tufts Solar Vehicle Battery Pack

Alan Deutsch, Rohan Harle, Aengus Kennedy
December 12, 2023

Table of Contents

Introduction

The Tufts Solar Vehicle Project (TSVP) is working to build a road-legal completely solar powered car to compete in national and global races. Fluid flow analysis is crucial for aeroshell design, but also for less obvious components like battery enclosures. Air flow through the battery enclosure has a strong influence on cell temperatures. If the 18650 Li-ion cells used in the car get too hot, they will degrade which can cripple the car's performance over long-distance races. According to American Solar Challenge (ASC) regulations[1], our battery enclosure must fulfill the following criteria in addition to controlling cell temperature:

1. Electrically isolate the cells from the chassis
2. Only forced exhaust is permitted
3. No external cooling (ie water cooling) is permitted

Cell cooling is determined mostly by the flow speed, the temperature of the air, and the enclosure geometry. It is important that the cells are kept as cool as possible and that there is minimal variation between cell temperatures (no hotspots). It is thus the goal of this report to understand, through fluid flow (lab 3) and heat transfer (lab 4) analysis, the performance of TSVP's current battery pack design and how it can be improved. After conducting our lab 3 analysis, we realized the design of the battery pack should be altered, so we used a new battery pack design in our lab 4 analysis, which was also a simpler geometry.

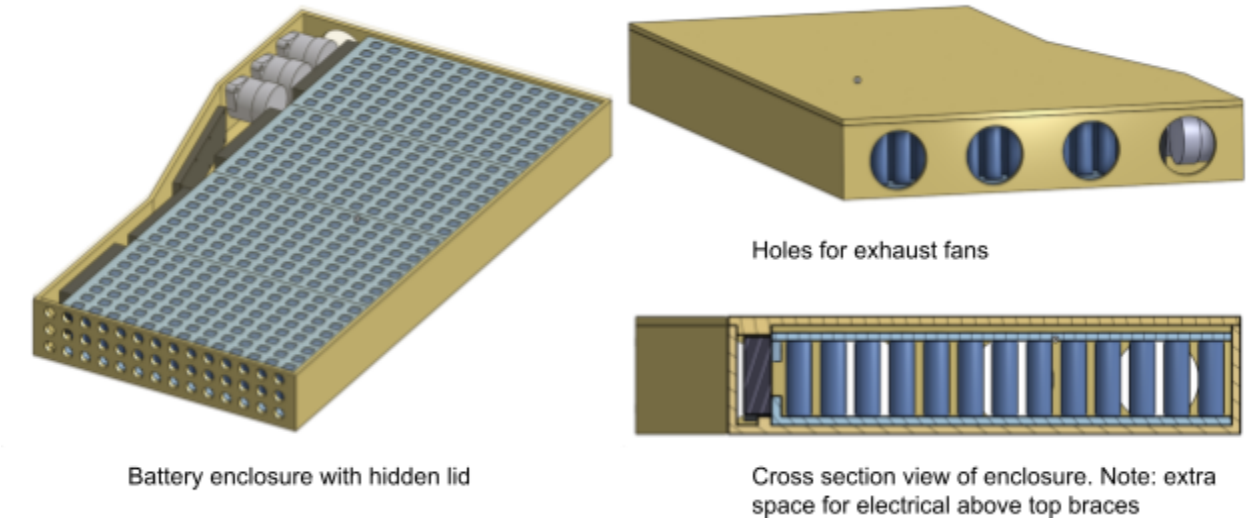

Figure 1: Render of Battery Pack CAD Design

For the fluid flow (lab 3) part of this report we attempt to determine how the initial battery box design shown above can be improved to maximize fluid flow velocity and flow uniformity. For heat transfer we try to determine the maximum cell temperature in the enclosure and the maximum temperature difference across cells in the enclosure.

Methods

Overall Geometry

The enclosure will be constructed of fiberglass sandwich panels with foam cores to provide structure and electrically insulate the cells. However, they aren't ideal since the core material thermally insulates the cells from the outside. The cells will be held together in arrays by braces in a shape determined by a variety of factors including the voltage and current requirements of the motor, the chassis shape, and ASC battery weight requirements. Placing the cells as far apart as possible is ideal to control temperatures in the enclosure, but due to space constraints, they have to be packed close together.

In order to understand the battery arrangement, we need to understand some battery terminology. A *pack* refers to the entire battery configuration consisting of cells and modules that supplies power to the car's electronics. A *cell* is the smallest possible form a battery can take, with voltage usually ranging from 1-6 V. In our case we are using 18650 cells, which have a diameter of 18 mm and height of 65 mm, and a voltage of 3.6 V and capacity of 3500 mAh[8]. A *module* consists of several cells connected in series or parallel. The pack is then assembled by connecting these modules together, also either in series or parallel. Connecting cells in series increases the voltage of the pack, connecting cells in parallel increases the capacity of the pack.

In our case, the motor of the car requires 115 V[4], which is equivalent to 32 18650 cells in series (3.6 V/cell * 32 cells = 115.1 V). To achieve this, we opted for four modules in series, each with eight cells in series. One of these eight cell groups is called a *string*. We then increased the strings in each module, which are connected in parallel, until we hit the weight limit of 20kg outlined in the ASC regulations[1]. We found the max number of strings in parallel to be 13. Thus the total pack configuration is 32 cells in series by 13 cells in parallel for a total voltage of 32 * 3.6 = 115.2 V and capacity of 3500 * 13 = 45.5 Ah.

Additional components that are critical for the batteries like the battery management modules and contactors are set off to the side. More details can be seen in the engineering drawing below.

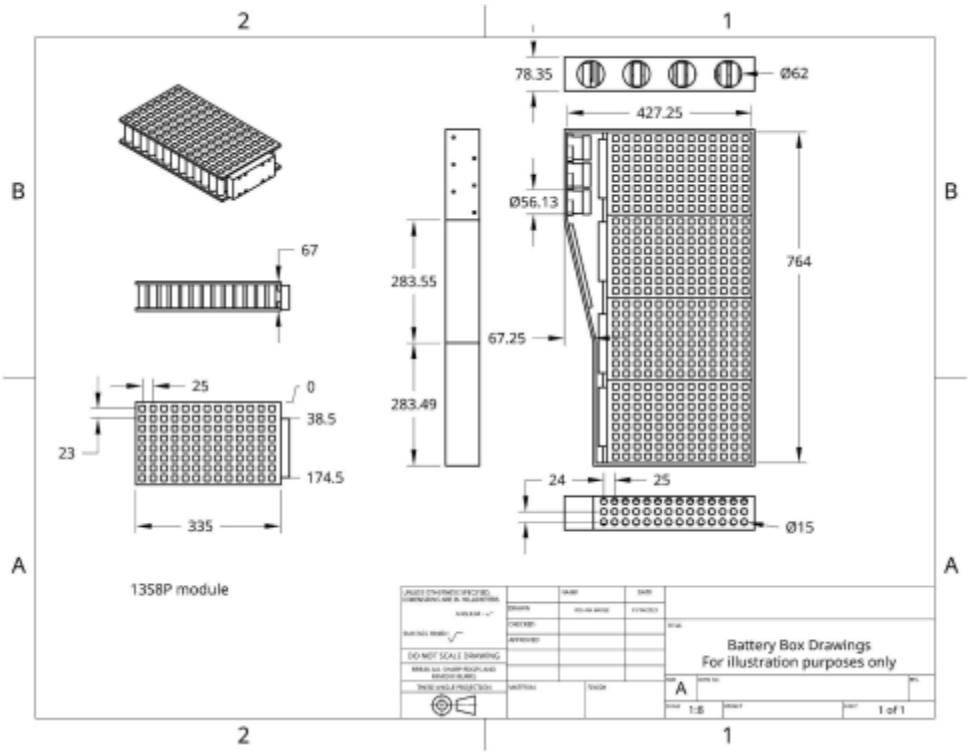

Figure 2: Engineering Drawing of Enclosure

We added exhaust fans to force flow through the enclosure and an array of holes for the intake to allow for air to move into the enclosure without compromising its structural integrity. After researching what other teams did [5], we decided to use 70mm brushless PC fans for the exhaust with a static pressure of 17.44 Pa and a free delivery flux of 0.008843 m^3/s[11].

Lab 3 Geometry

For lab 3, we decided to simulate flow through a 2-dimensional geometry that takes almost all of the complexity of the large, flat battery box into account rather than a 3-dimensional geometry that may not have converged. Using the original CAD model of the battery box as a reference, a 2D domain was created in COMSOL that reflected everything in the center cross section of the battery box including every battery, the four battery management units, and the three contactors. The geometry was meshed on the ‘coarser’ setting, and the complete mesh consisted of 148790 domain elements and 10844 boundary elements. The total simulation took **8 minutes and 15 seconds** to converge.

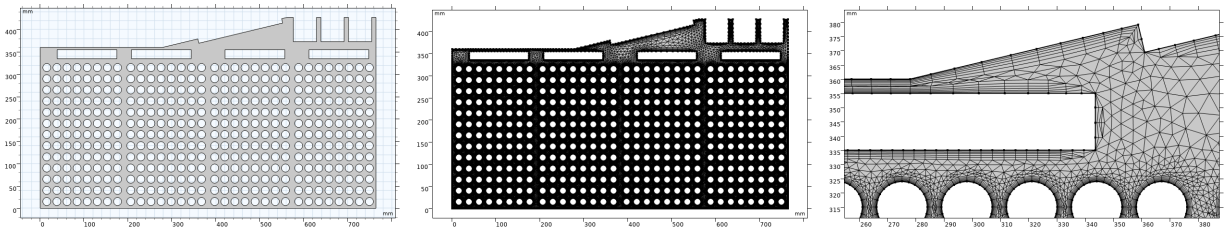

Figure 3: Multiple views of lab 3 geometry and mesh

Lab 3 Turbulent Flow Physics Model

We set up the simulation with inlet boundary conditions at atmospheric pressure along the left side of the geometry and a fan outlet boundary conditions along the right side of the geometry as shown above. Rather than specifying an exact flow rate or pressure difference at the fan boundary we entered the free delivery flux and static pressure specified in the datasheet of the brushless PC fans we use[11]. However, as will be elaborated on later, we made an error when defining the exit thickness of the PC fans.

The Reynolds number through a battery pack can be calculated using the diameter of the cell as the length scale[6]. The maximum velocity was approximated by first estimating the velocity flow rate. Assuming negligible negative pressure inside the enclosure, the flow through each fan is equal to the fan free volumetric flow rate. As will be shown later, this assumption may have been inaccurate as the negative pressure in the battery pack according to the 3D simulation is significant. Assuming inviscid flow which is unrealistic but sufficient for an approximation, the maximum velocity is equal to the total flow rate divided by the total area between the cells as shown below.

$$Q_{fan} = 0.008825417\frac{m^3}{s}$$

$$N_{fan} = 4$$

$$Q_{total} = N_{fan} \cdot Q_{fan} = 0.0353\frac{m^3}{s}$$

$$A_{betweencells} = \frac{(7 \cdot 63)}{1000^2}m^2$$

(7mm and 63mm are the dimensions of empty space between cells)

$$A_{total} = A_{betweencells} \cdot 13 = 0.005733m^2$$

$$U_{max} = \frac{Q_{total}}{A_{total}} = 6.2\frac{m}{s}$$

$$v_{air} = 16.92 \cdot 10^{-6}\frac{m^2}{s}$$ at 40 C

$$D_{cell} = 0.018m$$

$$R_e = \frac{U_{max}D_{cell}}{v_{air}} = 6551$$

Since the expected Reynolds number is greater than 2,000, we assumed turbulent flow. We selected the SST turbulence model because it was used in other studies to simulate similar air cooled lithium ion packs[3]. Irrespective of this, it makes sense to chose this model because it incorporates both the k-epsilon and k-omega models, which are both tried and true methods to predict turbulence, the primary difference being that k-epsilon is more accurate in the free stream and k-omega is more accurate closer to the boundary layer. Since our domain consists of both many boundary layers due to the tightly-packed cells and open spaces where flow can reach free stream velocity, SST makes sense as a model that accurately considers both of these flow types[9].

Lab 4 Simplified Geometry

The results of the lab 3 2D simulation showed us that flow was being directed away from the cells and into the auxiliary electronics area at the top of the battery pack. One of our main takeaways to improve cooling, therefore, was to block off the auxiliary electronics area for future versions of the battery pack. We incorporated this design change into our lab 4 heat transfer analysis. This also simplified the geometry significantly since now we can just model the pack as a simple rectangular box with the sides, top, bottom insulated and the front and back as the intake and exhaust respectively. To reduce the number of thin elements that may have hampered simulation convergence, we removed the small lip on the braces which hold the batteries in place. We decided to switch to a 3D simulation to better represent the inlet and outlet boundary conditions and to study temperature variation along the length of each cell.

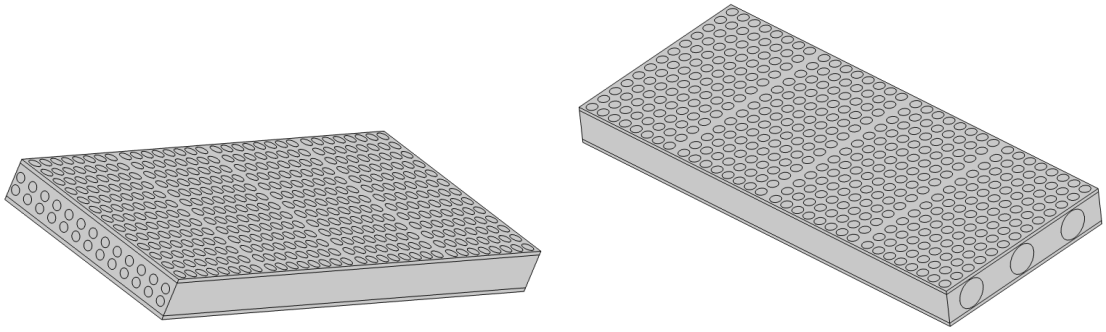

Figure 4: Views of overall lab 4 geometry

Lab 4 Heat Transfer Physics Model

Due to the relatively large size of our 3D model, we used an extremely coarse mesh in order for it to converge in a reasonable time. Instead of using the SST turbulence model as in the previous 2D flow simulation, we switched to the L-VEL turbulence model because it converges more quickly even though it sacrifices accuracy. However, it is still reasonable to use in internal flow electronic cooling [9]. For heat transfer, we selected the Kays-Crawford heat transport turbulence model which is appropriate for nonisothermal flow. Even with an extremely coarse mesh and a less computationally intensive turbulence model, our simulation took **54 minutes and 34 seconds** to converge.

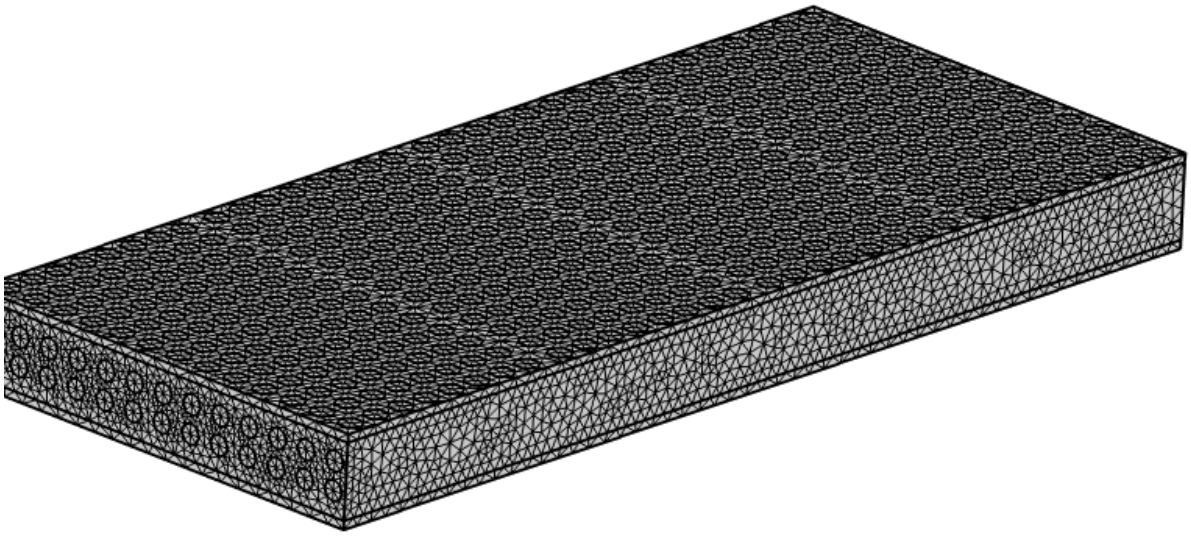

Figure 5: Extremely coarse mesh

In addition to the flow boundary conditions listed above, the thermal boundary conditions were added as shown in the figure below. It is reasonable to assume that the enclosure is thermally insulated because the thermal conductivity of the foam core is 0.028 W/mK[2]. Inflow and outflow heat transfer boundary conditions were defined at the inlet and outlet. The batteries and braces, the two solid domains, were assigned material properties as aluminum and acrylic respectively. Because we are only analyzing temperature at the surface of the cells, the exact material of the battery is less important.

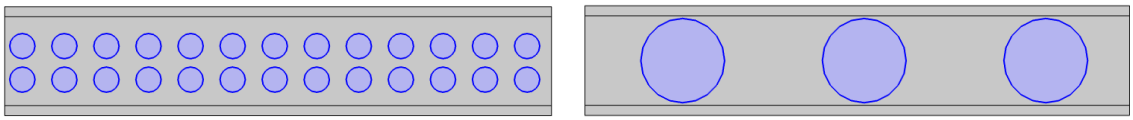

Figure 6: Inflow and outflow boundaries (flow and heat transfer)

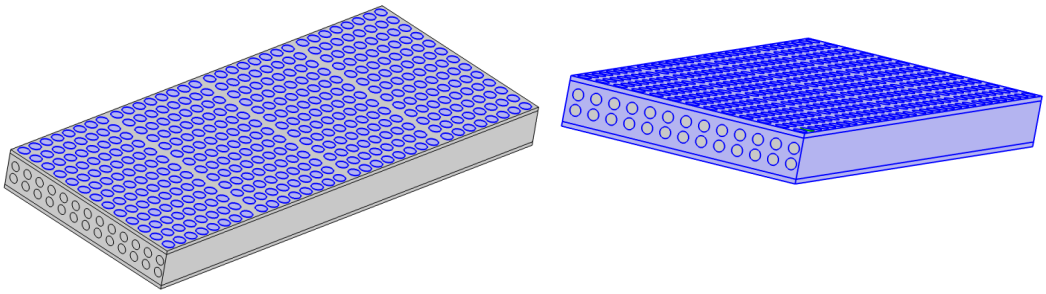

Figure 7: Heat sources (batteries) and thermal insulation.

Ambient temperature was set at 38C to reflect a worst case scenario. A heat source boundary condition was applied to each of the 416 cells. The heat generated by each cell (1.67W) was calculated based on the current flowing through each cell and the internal resistance of each cell as shown below.

Table 1: Parameters for calculating battery cell power output

Parameter Name	**Abbreviation**	**Value**
Maximum power draw	P_{motor}	5.0kW [4]
Nominal battery voltage	$V_{battery}$	3.6V [8]
Battery internal resistance	$R_{battery}$	150 milliohms [8]
Cells in series	C_{series}	32
Cells in parallel	$C_{parallel}$	13

Voltage across motor

$$V_{motor} = V_{battery} \cdot C_{series} = 115V$$

Current flow through motor

$$I_{motor} = \frac{P_{motor}}{V_{motor}} = 43.4A$$

Current flow through each battery

$$I_{battery} = \frac{I_{motor}}{C_{parallel}} = 3.33A$$

Heat generation by each battery

$$P_{battery} = R_{battery} \cdot I_{battery}^2 = 1.67W$$

Flow Results

2D Simulation (Lab 3) Results

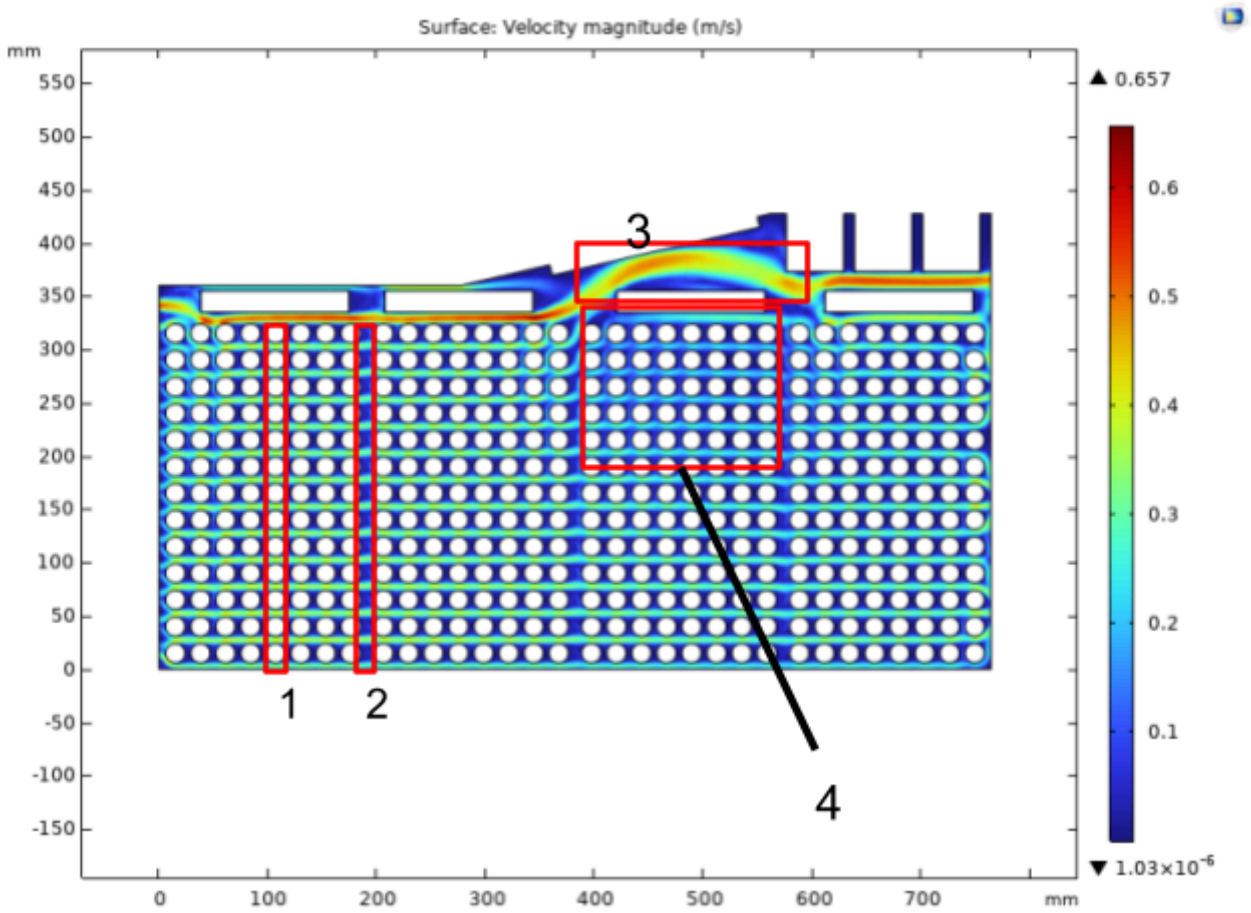

Figure 8: Velocity surface plot

As highlighted in annotations 1 and 2, the flow is faster between rows of cylinders than in the areas between modules due to conservation of flow rate, since the vertical cross-sectional area in the modules is less than between the modules. A significant amount of flow is diverted above the third battery management unit (BMU) from the left, which results in less flow through the batteries directly under it as well as the entire pack (annotations 3 and 4).

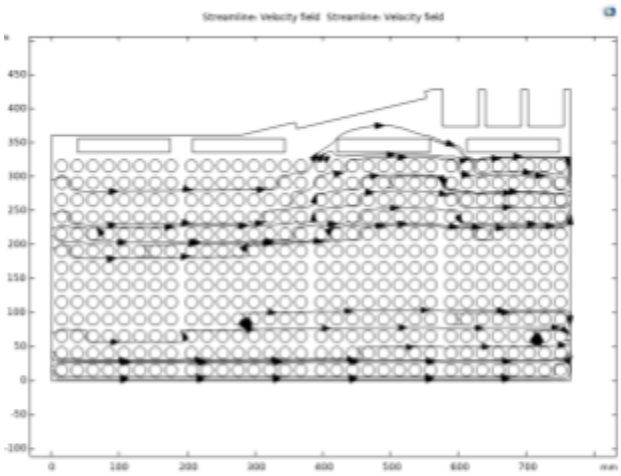

Figure 9: Streamlines due to flow through first and third fans (from bottom)

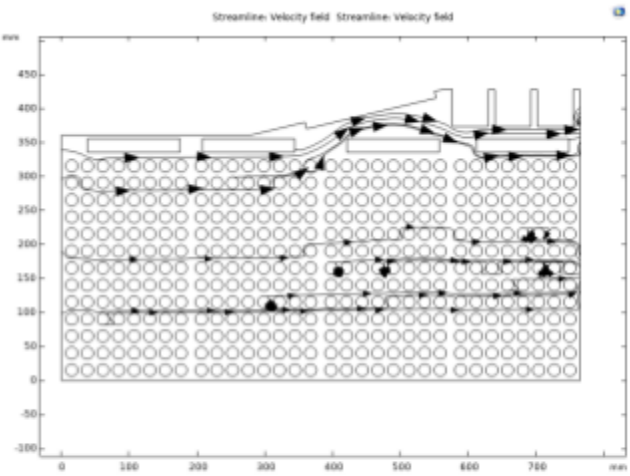

Figure 10: Streamlines due to flow through second and fourth fans

These plots describe the direction of flow as it moves from left to right through the domain. The flow due to the first and second fans passes through the cells going mostly straight across the domain. For the flow due to the third and fourth fans, however, we can more clearly see how the flow is being diverted upwards to the auxiliary electronics area and away from the batteries.

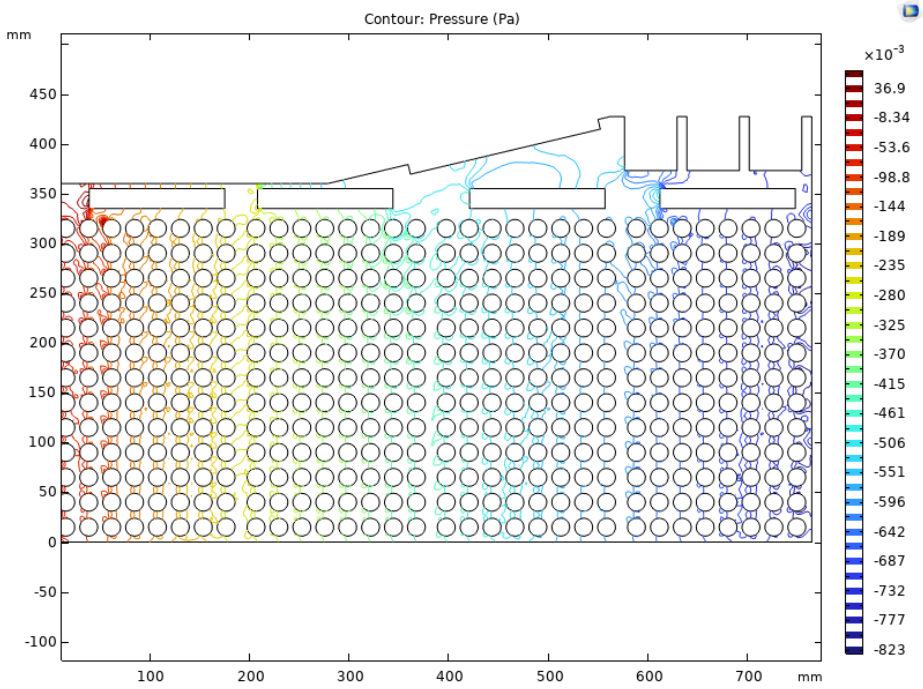

Figure 11: Contour Pressure Plot

This plot demonstrates how the pressure generally drops from left to right as the flow nears the fans. This makes sense because flow moves from regions of high to low pressure. We

can also see how the pressure in the region above the third BMU is low, which indicates how it is favorable for flow to enter said region.

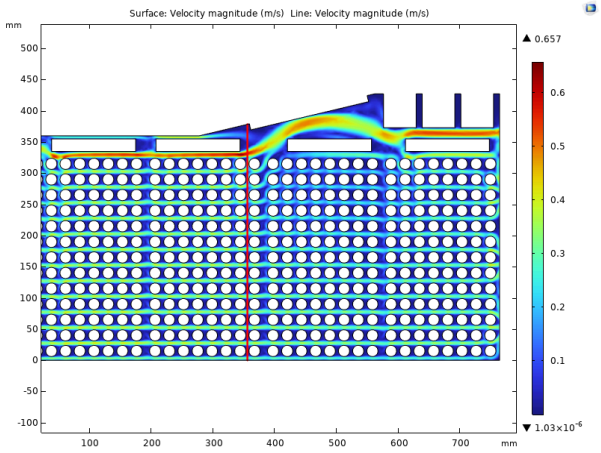

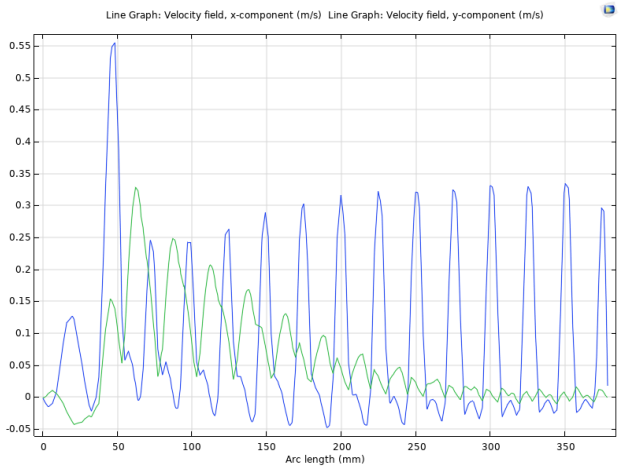

Figure 12: Velocity surface plot with vertical cut line (red) between two columns of batteries
Figure 13: X (blue) and Y (green) components of velocity along cut line

This plot shows the variation in velocity along a vertical slice through the domain between two columns of cells. It also slices through the flow that's diverted above the third BMU. As we can see, the vertical component of flow starts low at the top of the line, then jumps up as it reaches the space immediately to the left of the top right corner cell of the second module. This makes sense as the diverted flow at that point has a mostly upward trajectory. The vertical component then drops as we go further along the line as the flow is less influenced by the diversion.

For the x component, it too jumps as the line crosses the diversion, though slightly earlier, which makes sense as the flow above the two top right cells of the module has a high magnitude overall and is mostly horizontal in direction.

We can notice in both components that the velocity fluctuates between peaks and troughs that represent the spaces between rows of cells and in rows of cells, respectively. This again makes sense because flow is mostly horizontal so there is a lack of flow between columns of cells.

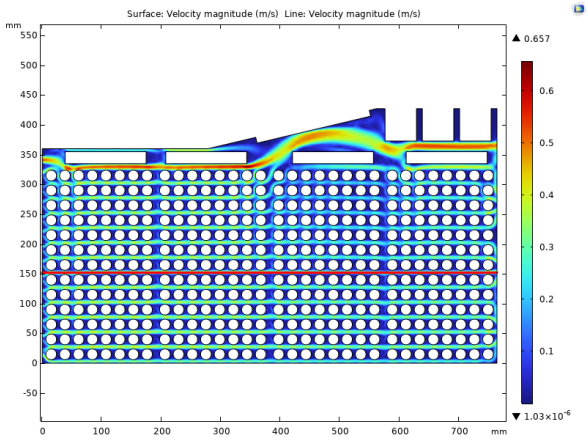

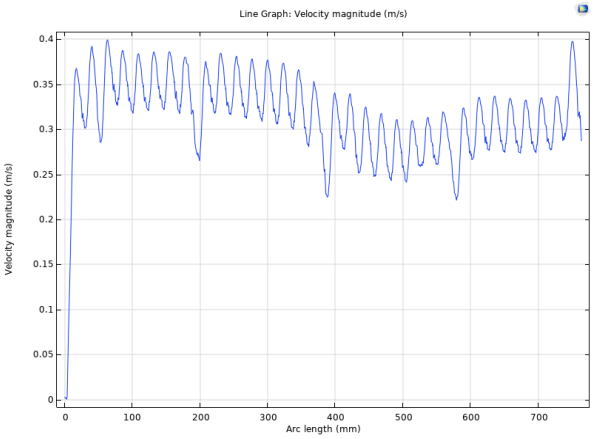

Figure 14: Velocity surface plot with horizontal cut line
Figure 15: Velocity magnitude along cut line

Lastly, we examine the flow along a cut line between two rows of cells roughly in the middle of the domain. We can see from this plot how the velocity of the flow stays relatively constant as we move from the left to the right of the domain. The major exception to this occurs in the third module, below the third BMU, which indeed has lower velocity due to the flow diversion.

The flow fluctuates similarly to the last plot between peaks and troughs representing the spaces in the cell columns and between the cell columns. This makes sense because the spaces in the cell columns are smaller, and thus have higher velocity, than the spaces between cell columns.

3D Simulation (Lab 4) Results

After concluding that battery cooling would be improved by blocking off the auxiliary electronics area, we decided to adjust our geometry as stated in the “Lab 4 Simplified Geometry” section. The following plots depict the change in flow after transitioning to a 3D simulation and eliminating flow diversion to the auxiliary electronics.

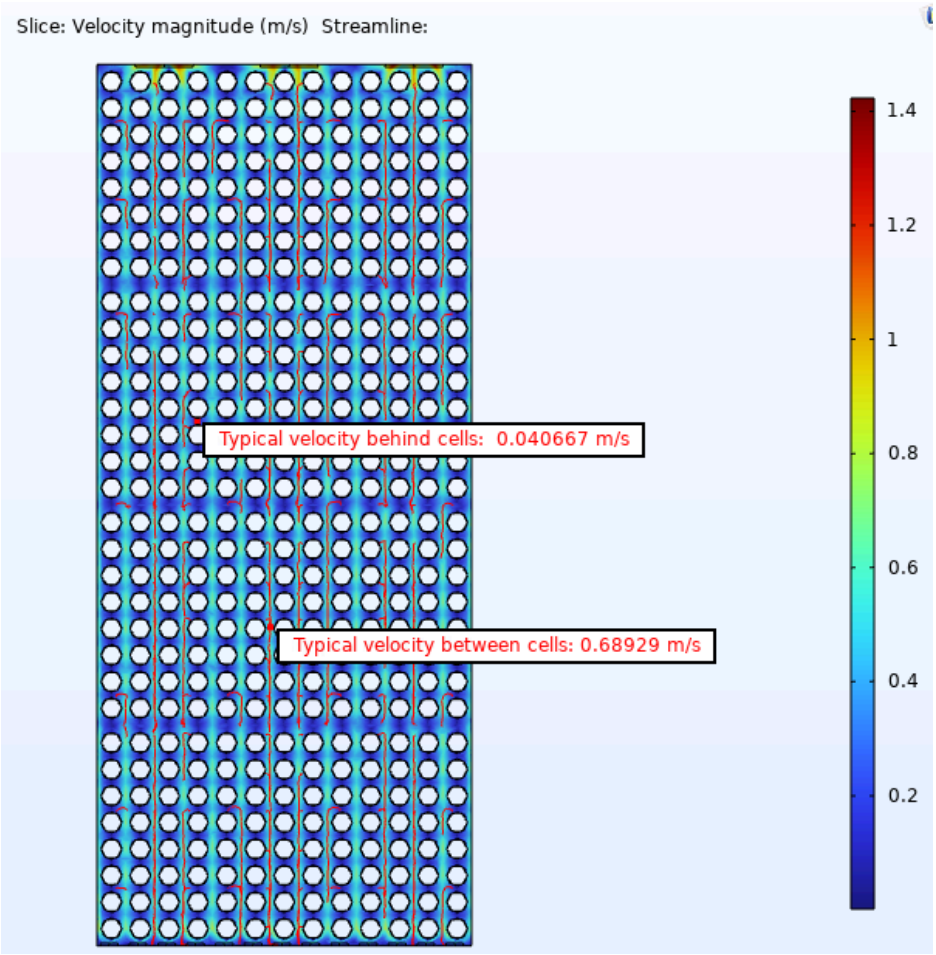

Figure 16: Top down velocity plot through center of 3D simulation with red streamlines and typical velocity values

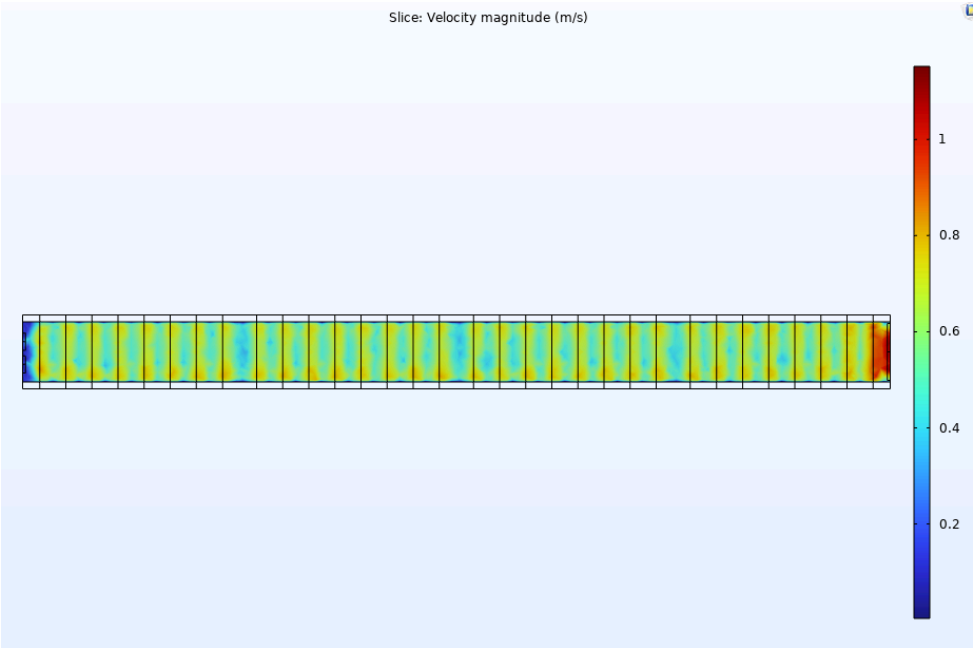

Figure 17: Side view velocity slice plot through center of 3D simulation

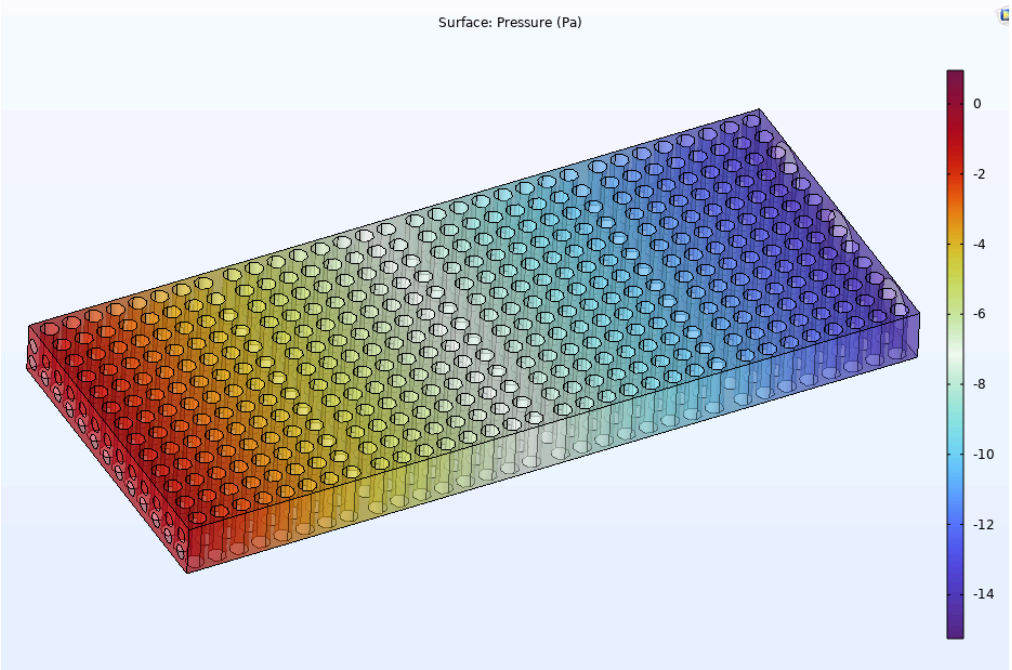

Figure 18: Isometric view pressure surface plot of 3D simulation

When first calculating the Reynolds number to determine whether the flow was laminar or turbulent we assumed that the pressure drop across the battery pack was negligible. This assumption was valid for the 2D analysis with flow being diverted to the auxiliary electronics area. However, when the auxiliary electronics area was blocked off for the 3D flow simulation, the pressure drop became significant at 14 Pa at the exit as shown above. This is close to the fan static pressure of 17.44 Pa causing the fan outlet velocity to reduce but less so than when the velocity was diverted in the 2D analysis. This explains why the typical velocity (Fig.16) between the cells of 0.689 m/s is an order of magnitude less than the velocity determined in the preliminary Reynolds number calculation (6.2 m/s), which assumed the fan was operating against zero static pressure. Indeed, calculating the Reynolds number based on the velocity from the 3D simulation suggests that the flow is laminar and not turbulent.

Flow Validation

In 1939, Lindsey conducted an experimental investigation of drag forces experienced by cylinders under flow conditions with widely varying Reynolds numbers[13]. In NACA's 11-inch high-speed wind tunnel, polished cylinders and prisms of various dimensions were mounted on a recording spring balance, allowing precise measurement of the drag forces they experienced during a variety of airflow velocities. The fluid flow results of our simulation can be validated by Lindsey's results using an integral measurement of the forces on the simulated battery cylinders in COMSOL.

A free-stream velocity quantity is necessary to find the coefficient of drag of the simulated cylinders. In our boundary geometry, an effective free-stream velocity can be calculated by normalizing the inlet velocity by the proportion of inlet area to total pack frontal area as follows.

Table 2: Parameters for calculating free-stream velocity

Parameter name	**Abbreviation**	**Value**
Average inlet velocity	V_{inlet}	0.866 m/s
Number of inlets	N_{inlets}	26
Area of single inlet	A_{inlet}	0.000177 m^2
Total battery pack frontal area	$A_{frontal}$	0.0172 m^2

The effective free-stream velocity for our study can then be calculated using this relation

$$V_{study} = V_{inlet} \cdot \frac{(N_{inlets} \cdot A_{inlet})}{A_{frontal}} = 0.231 m/s$$

This new free-stream velocity suggests a new Reynolds number

$$Re_{new} = \frac{V_{study} D_{cell}}{v_{air}} = 259.875$$

As discussed above, this new lower Reynolds number indicates that the flow is laminar and that the cylinders will experience more drag than they would if the flow were turbulent. At this Reynolds number, Lindsey's study found a drag coefficient of 1.3. In COMSOL, integrals on seven of the front cylinders evaluating the drag force divided by the frontal area, the density of air, and half the free-stream velocity squared returned coefficient of drag values between 1.279 and 1.376, averaging 1.337. The close agreement of these two numbers are strong evidence of the validity of our simulation. Our calculation that the air flow is more laminar was supported, as these numbers are also close to 1.2, the textbook's suggested coefficient of drag for laminar flow over a cylindrical cross section.

The simulation could be validated more strongly by an experimental study of airflow through a whole grid of cylinders or by a study with data about other comparable quantities about flow around a cylinder, but to our surprise, after extensive searching for such experiments, we did not find any.

Heat Transfer Results

Heat Transfer Results

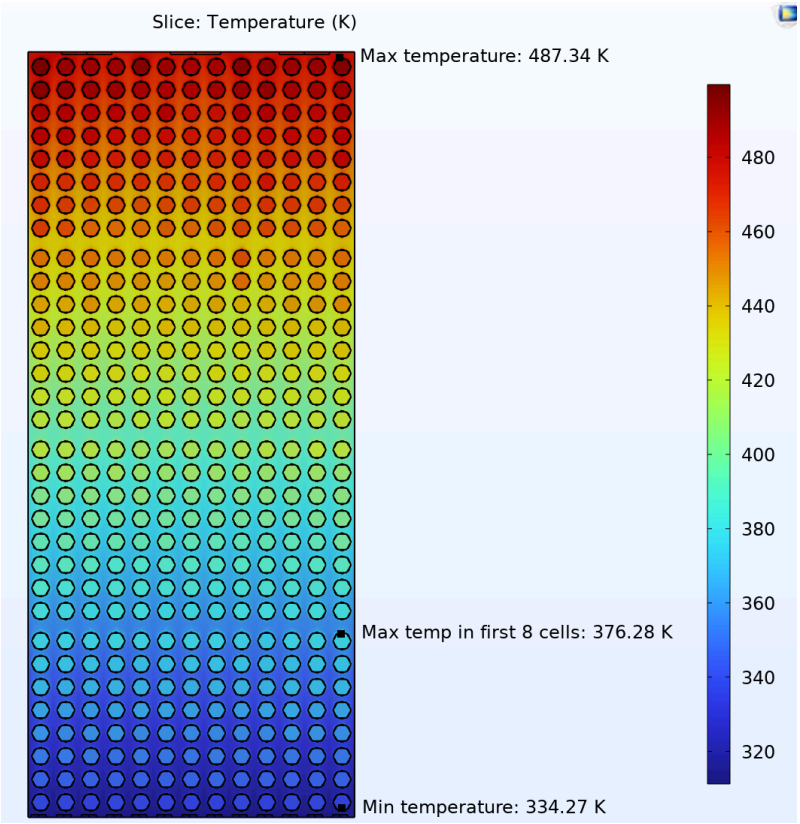

Figure 19: Temperature slice plot 1

We generated the plot above by plotting a slice through the center of the cells. It shows temperature variation across the array with the maximum and minimum temperatures probed. We also probed a cell at the end of the first module for use in the validation section below. The maximum temperature near the outlet is 487 K or 214 C and the minimum temperature of one of the cells at the inlet is 86 C.

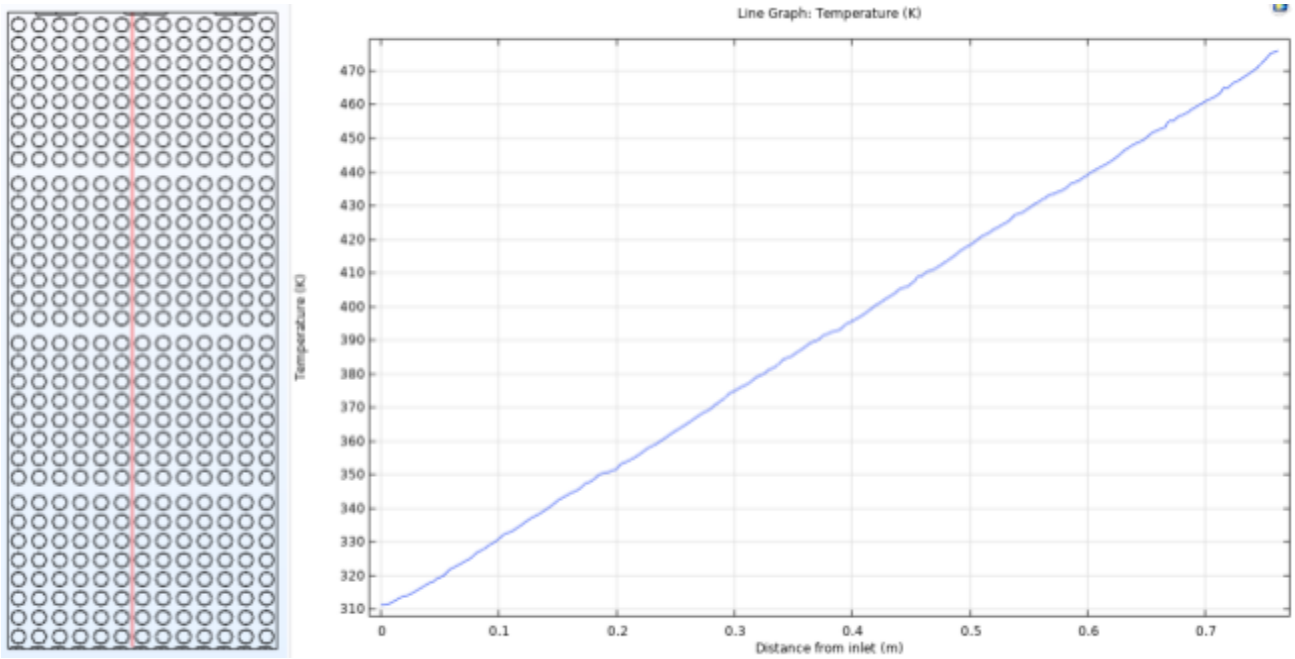

Figure 20: Temperature versus distance from inlet along the center of the battery pack

The figure above highlights how the fluid temperature between the cells increases as it flows from the inlet to the outlet. For every centimeter, the temperature increases by approximately 2.3 C.

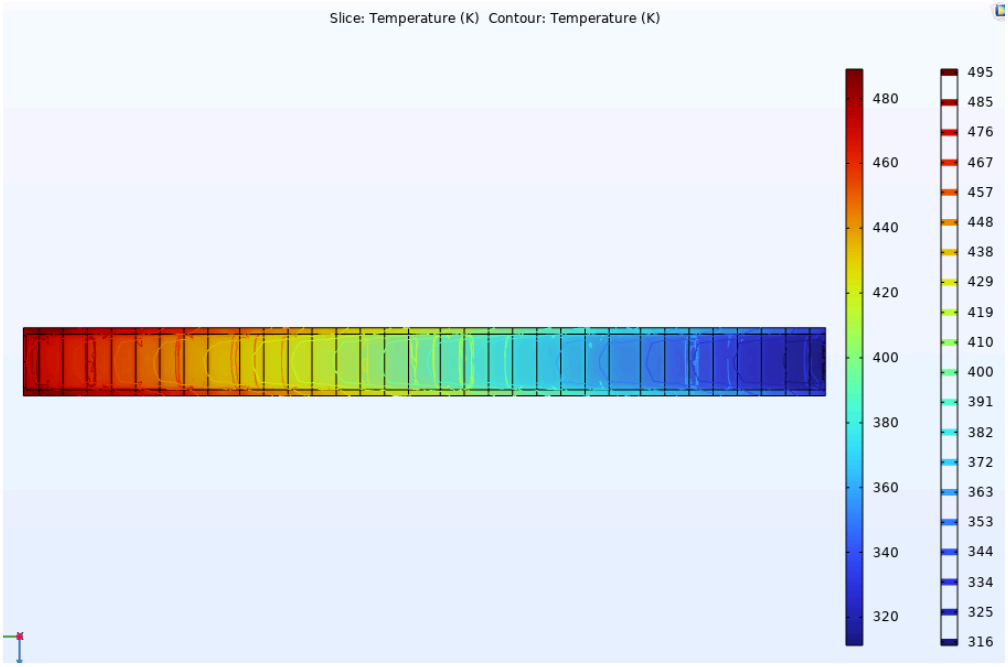

Figure 21: Temperature slice plot 2

We also plotted temperature across the length of the cells with another slice plot. The temperature across the length of the cells is fairly uniform. However, the contour plots highlight

the thermal boundary layers that form at the top and bottom of the pack where the fluid contacts the battery braces which have been heated.

Heat Transfer Validation

Fan et al. conducted an extensive experimental study on 18650 cells where they varied discharge rate, air inlet temperature, inlet velocity, and cell arrangement[10]. For each experiment, they recorded the maximum temperature rise and maximum temperature difference across cells. These are the same parameters that we studied in our simulations. Similar to our simulation, this trial blew air across the cylindrical bodies of the batteries, while their flat top and bottom faces were not actively cooled, but it is unclear if they are insulated as was assumed in our simulation. Their testing setup is shown below.

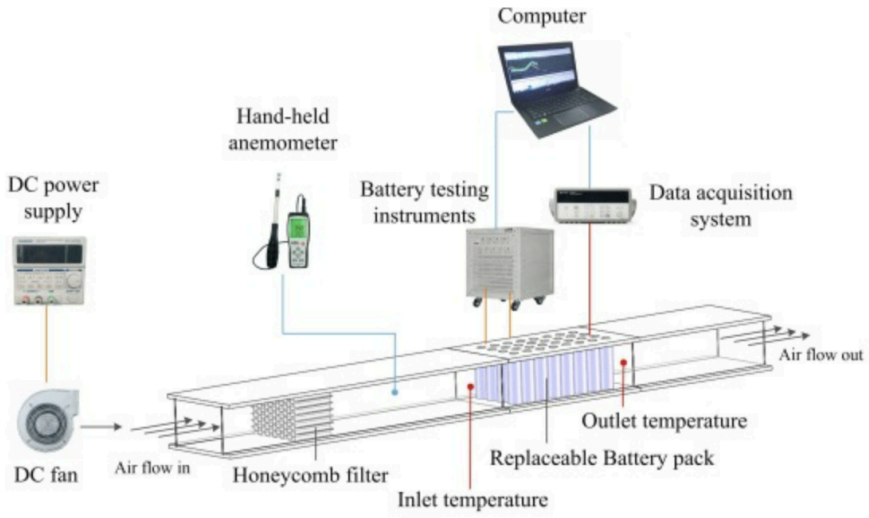

Figure 22: Experimental setup in validation paper [10]

The batteries had a nominal voltage of 3.6V and nominal capacity of 3.50 Ah which perfectly matches the batteries we plan to use in the solar car battery pack. Unfortunately, the equivalent resistance, a key variable for determining the heat generation by each cell, was not included in the listed parameters for the 18650 cells used in their experiment. The spacing between the center of each cell was 22mm which is similar to the 25mm spacing in our current battery pack design. Lastly, Fan et al. tested at a 1C discharge rate which matches the maximum discharge rate that we determined based on the maximum power draw from our motor.

However, unlike our battery box design which has forced outlet flow and grid of inlet holes, Fan et al. used a DC fan and honeycomb filter to ensure uniform forced flow into the cells. This made it necessary to calculate what our effective flow would be if it were spread out over the frontal area of the cell instead of being channeled through the inlet holes. In the fluid validation section, we determined an equivalent velocity for comparison to the study by multiplying the average inlet velocity (calculated using a surface average in COMSOL) by the ratio of the total inlet area to the frontal area of the battery box to find an effective velocity of 0.213m/s. This equivalent velocity is significantly less than the lowest experimentally tested

velocity of 0.6 m/s. The table below summarizes the key similarities and differences between the validation study and our simulation.

Table 3: Comparison between validation study and our simulation assumptions

	Fan et al. key assumptions	**Our CFD assumptions**
Discharge rate	1C/3.5A	0.95C/3.33A
Cell resistance	Unknown	150 milliohms
Cell spacing	22 mm	25 mm
Velocity	0.6 m/s	0.231 m/s (equivalent velocity)
Ambient temperature	30 C	38 C

With this key difference in mind, the summary of our results and theirs are outlined in the table below. The maximum temperature rise relative to ambient temperature ($\Delta T_{rise,max}$) and maximum temperature difference across cells (ΔT_{max}) for the simulated results were calculated by only considering the first module which is 8 cells deep (matches the experimental setup).

Table 4: Comparison between validation and our simulation results

	Fan et al. results	**Our CFD results**
$\Delta T_{rise,max}$	12.5 C	65.13 C
ΔT_{max}	6 C	42.01 C

A preliminary comparison of experimental and simulation results indicates that our simulation is not accurate as they differed by over a factor of 4. However, as stated above, the two setups vary in a few key ways which may have contributed to this large discrepancy. Most importantly, the equivalent velocity in our simulation of 0.231 m/s is approximately one third as large as the experimental results which would significantly reduce the convective heat coefficient between the batteries and the air, thus contributing to the higher temperatures in our simulation. As shown in the flow validation section, the velocity is slow enough to make it laminar. When compared to the turbulent flow achieved by Fan et al., the laminar flow in our study would mix hot and cool air less effectively and increase the temperature in the battery pack. In addition, our ambient temperature was slightly higher than theirs. This preheated air is less effective at cooling the cells. In addition, it is unclear if the top of their pack is insulated as assumed in our simulation. Lastly, it is likely that the batteries used by Fan et al. had a significantly lower internal resistance than the assumed resistance in our simulation of 150 milliohms. The datasheet for the batteries we used indicated that the internal resistance for each

cell is less than or equal to 150 milliohms so it is possible that the cells used in the Fan et al. study had a resistance closer to 100 milliohms.

Given the multitude of factors that explain the higher temperatures observed in our simulation compared with the results by Fan et al, we can conclude that our results are likely valid. However, additional analysis could be helpful to properly validate or reject our simulated results. For example, a separate simulation with the same ambient temperature, flow velocity and cell configuration (4x8) could be compared more definitively with the results from Fan et al.

Conclusions and Future work

Flow Conclusions

In response to our flow question, we determined that the additional electrical components area significantly reduces fluid velocity through the cells. In the future, the battery pack should be redesigned to physically block air from moving into that area, thus maximizing fluid flow velocity and heat transfer through the cells. We incorporated this finding into the geometry we used for our lab 4 investigation, and found that the altered design indeed improves flow velocity through the cells. At a point roughly in the middle of the pack, fluid velocity increased from 0.35 to 0.68 m/s, for example.

From our lab 3 investigation we also concluded that velocity uniformity through the cells could be improved as well. We found that air flowed much faster (~0.4m/s) between rows of cells and stagnated between cells in a row. These areas of slow recirculating flow would likely heat up and reduce heat transfer to the fluid. One possible solution is staggering the cells.

The fluid flow exerted drag on the batteries at a magnitude in very close agreement with experimental data on fluid flow around a cylinder, so our confidence in the validity of the fluid flow simulation is high. Regarding the validity of our initial Reynolds number calculation, for both the 2D and 3D flows we found that the pressure drop across the battery pack was not negligible (-14 Pa). This reduced the effectiveness of the fan resulting in considerably slower flow between the cells than we originally predicted when calculating the preliminary Reynolds number, which assumed no pressure drop across the battery pack. Thus, a goal for future designs is to further increase the flow speed through the cells which will improve convective heat transfer both by increasing flow velocity and making the flow regime turbulent.

Heat Transfer Conclusions

Our questions going into the heat transfer investigation were to 1) determine the maximum cell temperature in the enclosure and 2) the maximum temperature difference across cells in the enclosure. We found the maximum temperature in the battery pack to be 213 C and the maximum temperature difference across the cells to be 153 C. This maximum temperature of 213 C is well above the permissible battery temperature of 60 C [10], so the battery pack should be redesigned if our study is valid. Although our simulated results differed significantly from the results of the validation study, the differences in flow velocity, ambient temperature, boundary conditions, and battery internal resistance likely account for these differences. Thus,

we can conclude that our simulation is indeed valid, and thus the battery pack should be redesigned.

Although the simulation itself might be valid, the input variables might be inaccurate. Our study was set up as time-independent/steady-state, and we used values corresponding to the peak power output of the batteries. Thus, the simulation is representing a scenario where the battery pack has heated up to such an extent that the energy going into the pack is the same as the energy leaving it. It could be the case that the battery temperatures simulated in such a scenario are much higher than the average working temperatures encountered in practice, where the motor isn't continually drawing maximum power from the batteries.

In the future there are a few changes we could make to improve the accuracy of our CFD results. For one, we used one of the least computationally demanding turbulent flow models, L-VEL, which is less accurate than SST, which we used in the 2D CFD. Additionally, we used an extremely coarse mesh. Still, we believe the overall setup to represent the flow situation well, and the battery temperature is well over the upper limit, thus we can be confident that a design change is warranted.

Although the study could be improved as described above to make the temperature data more accurate, it isn't worth it because we already know from the existing study that the design of the enclosure should be improved so that the flow through the pack becomes faster/turbulent. After redesigning the enclosure, we can then run the study with the more accurate modifications described in the previous paragraph, such as SST, a finer mesh, and also a time-dependent analysis.

Improvements to Design

1. Increase heat transfer coefficient and transition to turbulent flow with more/higher power fans
2. Decrease length of enclosure, or stack cells vertically
3. Stagger cells to improve flow uniformity (reduce stagnant flow behind cells)
4. Reduce negative pressure gradient to improve fan effectiveness
5. Select batteries with a lower internal resistance to reduce heat generation

Citations

[1]American Solar Challenge, “2024 Regulations,” no. Release B. pp. 26–32, Oct. 08, 2022. Accessed: Dec. 12, 2023. [Online]. Available: https://www.americansolarchallenge.org/ASC/wp-content/uploads/2022/10/ASC2024-Regs-EXTERNAL-RELEASE-B.pdf

[2]DIAB Group, “H Manual.” p. 25. Accessed: Dec. 12, 2023. [Online]. Available: https://www-eng.lbl.gov/~ecanderssen/Composite_Design/Divynicell/H_Man_M.pdf

[3]L. H. Saw, Y. Ye, A. A. O. Tay, W. T. Chong, S. H. Kuan, and M. C. Yew, “Computational fluid dynamic and thermal analysis of Lithium-ion battery pack with air cooling,” *Applied Energy*, vol. 177, pp. 783–792, Sep. 2016, doi: 10.1016/j.apenergy.2016.05.122.

[4]Marand, “Solar Car Wheel Motor Information Sheet ,” *Marand Electric Solar Car In-Wheel Motors* . [Online]. Available: https://ia804703.us.archive.org/20/items/pdfy-vz9FEuZIaOhE-jjQ/Solar%20Car%20Wheel%20Motor%20Information%20Sheet.pdf

[5]M. Srimongkolkul, “KU solar car team battery pack design,” *Michael Srimongkolkul Blog*, Oct. 11, 2020. https://michaelsri.wordpress.com/2020/10/11/kusolarcar-batterypack/ (accessed Nov. 14, 2023).

[6]N. Yang, X. Zhang, G. Li, and D. Hua, “Assessment of the forced air-cooling performance for cylindrical lithium-ion battery packs: A comparative analysis between aligned and staggered cell arrangements,” *Applied Thermal Engineering*, vol. 80, pp. 55–65, Apr. 2015, doi: 10.1016/j.applthermaleng.2015.01.049.

[7]T. Wang, K. J. Tseng, J. Zhao, and Z. Wei, “Thermal investigation of lithium-ion battery module with different cell arrangement structures and forced air-cooling strategies,” *Applied Energy*, vol. 134, pp. 229–238, Dec. 2014, doi: 10.1016/j.apenergy.2014.08.013.

[8]US Electronics, “Li-ion Cylindrical Battery Cell Specification.” May 02, 2021. Accessed: Dec. 12, 2023. [Online]. Available:

https://mm.digikey.com/Volume0/opasdata/d220001/medias/docus/2587/USE-18650-3500mah%20Rev2022.pdf

[9]W. Frei, “Which turbulence model should I choose for my CFD application?,” *COMSOL*, Jul. 06, 2017. https://www.comsol.com/blogs/which-turbulence-model-should-choose-cfd-application/ (accessed Dec. 12, 2023).

[10]Y. Fan, Y. Bao, C. Ling, Y. Chu, X. Tan, and S. Yang, “Experimental study on the thermal management performance of air cooling for high energy density cylindrical lithium-ion batteries,” *Applied Thermal Engineering*, vol. 155, pp. 96–109, Jun. 2019, doi: 10.1016/j.applthermaleng.2019.03.157.

[11]GDSTIME Store, “GDSTIME 12V DC 3PIN 70mm Fan, 70mm x 70mm x 25mm Brushless Cooling Fan : Electronics,” *Amazon*. https://www.amazon.com/GDSTIME-3PIN-70mm-Brushless-Cooling/dp/B013HOJJWU/ref=sr_1_10?crid=3SSALVCKWQUOA&keywords=70mm%2Bpc%2Bfan&qid=1702413230&sprefix=70mm%2Bpc%2Bfan%2Caps%2C73&sr=8-10&th=1 (accessed Dec. 12, 2023).

[12]W. F. Lindsey, "Drag of Cylinders of Simple Shapes," *Twenty-Fourth Annual Report of the National Advisory Committee for Aeronautics*, pp. 169-176, Jan. 09, 1939. Accessed: Dec 12, 2023. [Online]. Available: https://www.google.com/books/edition/Annual_Report_of_the_National_Advisory_C/3vg6dJSmQ1oC?q=drag+coefficient+cylinder+experiment&gbpv=1#f=false

Lab 3 Research

Journals:

- Thermal performance analysis of 18,650 battery thermal management system integrated with liquid-cooling and air-cooling - ScienceDirect
- Thermal investigation of lithium-ion battery module with different cell arrangement structures and forced air-cooling strategies - ScienceDirect
- Computational fluid dynamic and thermal analysis of Lithium-ion battery pack with air cooling - ScienceDirect
    - Recommends SST Turbulence model
- Shortcut computation for the thermal management of a large air-cooled battery pack - ScienceDirect
- Multiobjective optimization of air-cooled battery thermal management system based on heat dissipation model | SpringerLink
- Passive thermal management of the lithium-ion battery unit for a solar racing car - Celik - 2019 - International Journal of Energy Research - Wiley Online Library

Best Journals:

- Fluid flow analysis - only CFD
- 2x2 experimental flow - only CFD
- Good heat transfer - only simulation, not experimental
- https://www.sciencedirect.com/science/article/pii/S2352152X23023812
- https://www.sciencedirect.com/science/article/pii/S1359431118376695 - lots of temperature data, no velocity - cited for heat transfer validation
    - All in C:
    - $\Delta T_{rise,\ max}$: 5
    - ΔT_{max}: 3
    - $\Delta T_{rise,\ avg}$: 4
    - $\sigma \Delta T_{rise,}$: 1
    - Anemometer measured airflow through the batteries

Turbulence models article:
https://www.comsol.com/blogs/which-turbulence-model-should-choose-cfd-application/

Battery design in comsol: https://www.youtube.com/watch?v=K4GzQxDyd-k

Batteries resource from TSVP: Battery box design - Google Docs

KU Solar Car Team Battery Pack Design – Michael Srimongkolkul (wordpress.com)

Boundary conditions:

- Inlet at entry
    - Molar volume: molar mass/density = 0.028959 kg/mol/1.160701 kg/m³ = 0.02495
    - Temperature of air: 38 celsius

- Fan at exit
    - how to model
    - 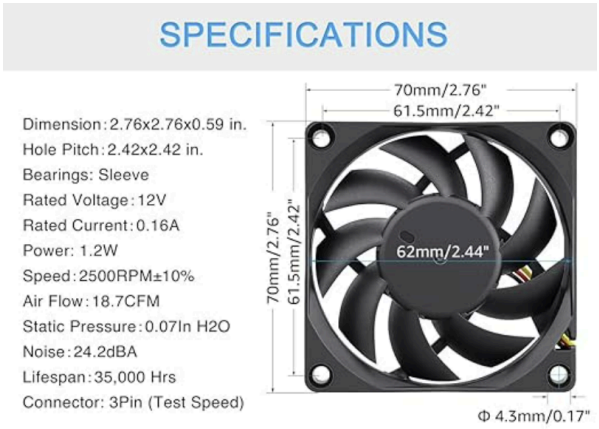

    - Volumetric flow rate: 0.008825417315 m^3/s
    - Static pressure: 17.4357 Pa
    - How to choose better fans:
        - Fan Selection & Application Guide - Electromechanical / Fans, Thermal Management - Electronic Component and Engineering Solution Forum - TechForum | Digi-Key (digikey.com)
        - Fan & System Curves - Electromechanical / Fans, Thermal Management - Electronic Component and Engineering Solution Forum - TechForum | Digi-Key (digikey.com)

Battery boundary conditions;

- General battery information
    - 18650 shape
    - 3.7 V
    - 3500mAh
    - Draws 4.5A through each battery (calculated below)
    - 1.286 C discharge rate
- constant heat flux
- W=RI^2 where I = 10A max current, R = 0.150 ohms
    - Actual rea of cell: 0.00418 m^2
    - W = 3.0375 watts
    - Q_{actual} = 726 W/m^2
    - Area of cell in 2D simulation assuming depth of 1m: 0.057 m^2
    - Q_{2D} = 53.24 W/m^2
- motor draws maximum 5kW, 138 V gives 36A
- current configuration 8 cells in parallel 36/8= 4.5A through each battery
- Internal resistance: less than or equal to 150 milliohms Source: Specifications (digikey.com)
- Target temps: Experimental study on the thermal management performance of air cooling for high energy density cylindrical lithium-ion batteries - ScienceDirect
    - 20-40C is optimal

    - -20-60 is permissible
    - Max temp difference should be 5C

Battery CAD:
21700 8S9P module | Battery box (onshape.com)

Fan research
- https://techcompass.sanyodenki.com/en/training/cooling/fan_basic/004/index.html#:~:text=Airflow%20indicates%20the%20volume%20of,equipment%20with%20high%20mounting%20density.
- https://www.cgdirector.com/pc-fan-airflow-direction/
-

Lab 4

Flow validation:
- Annual Report of the National Advisory Committee for Aeronautics - United States. National Advisory Committee for Aeronautics - Google Books
    - report no. 619 on page 169
    - our Reynolds number is 6551 - page 171predicts precisely 1.2
    -
-

Battery box materials:

- Thermal conductivity of foam core (H 45): 0.028 W/mK
- Thermal conductivity of fiberglass (Table 5.5): 0.28 W/mK

Strategies to get convergence:
- Add complexity in stages
- Consider mesh quality
- L-VEL for preliminary analysis

Decisions:
- Define heat flux across cell boundary or model convection and power dissipation

Temperature of air: 40 celsius (worse case scenario)

Iterative process:

- Flow analysis
    - 2D simulation of small section
    - 2D simulation of entire geometry
        - Learned that extra electronics need to be blocked off
        - Consider staggering cells
        - Learned how to use fan boundary conditions
    - Simplified 1:3 3D simulation w/ simple velocity defined outlet and pressure defined inlet
        - L-VEL model with extra coarse mesh to reduce solve time (even though less accurate). Enough to verify if setup is correct
        - SST model with coarse mesh to ensure that SST model with coarse mesh will converge as well
    - Simplified geometry of entire pack
        - Doesn't include extra electronics area since we are blocking that off
        - L-VEL model with extra coarse mesh to verify symmetry boundary conditions. Verify setup - 19 minutes and 27 seconds
        - Repeat with finer mesh and SST for more accurate results
- Heat transfer analysis
    -

Directions

1. Ask a useful question about heat transfer that relates to your flow of choice and can be answered with CFD.
    - What is the max temperature across battery pack
    - How much heat flux is removed by the fans?

2.

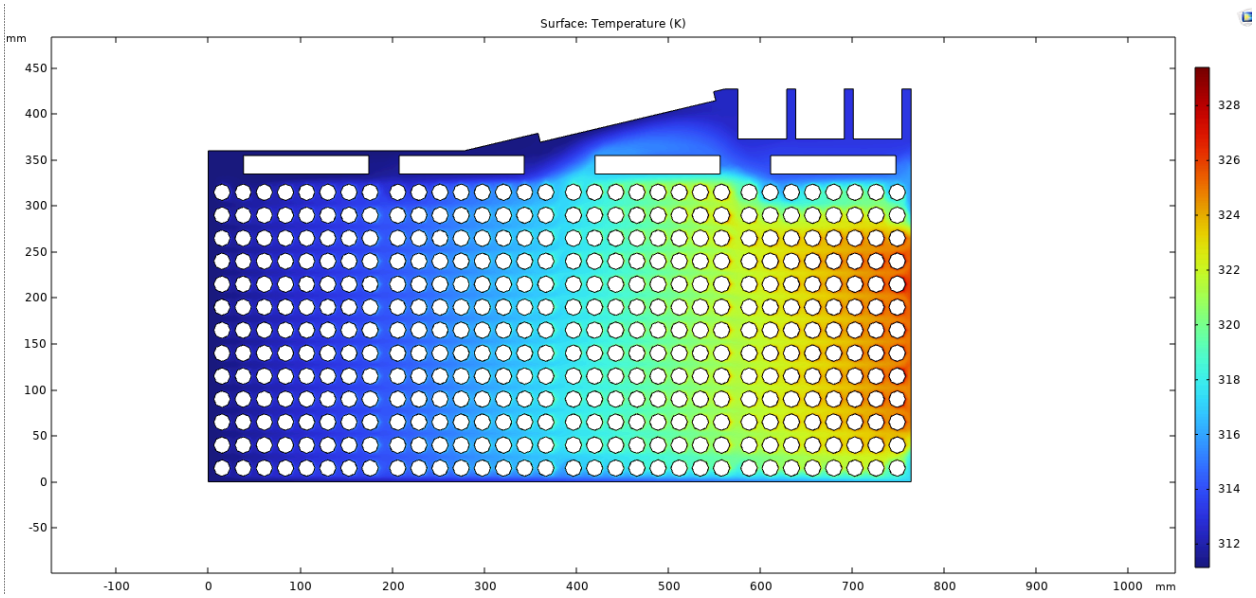
Surface: Temperature (K)
mm
450
400
350
300
250
200
150
100
50
0
-50
-100
0
100
200
300
400
500
600
700
800
900
1000
mm
328
326
324
322
320
318
316
314
312